Received: 24 April 2020 | Revised: 15 July 2020 | Accepted: 19 July 2020

DOI: 10.1111/cbdd.13766

RESEARCH ARTICLE

WILEY

Structure-based non-nucleoside inhibitor design: Developing inhibitors that are effective against resistant mutants

Steven J. Smith[1] | **Gary T. Pauly**[2] | **Katharine Hewlett**[1] | **Joel P. Schneider**[2] | **Stephen H. Hughes**[1]

[1]HIV Dynamics and Replication Program, Center for Cancer Research, National Cancer Institute, Frederick, MD, USA

[2]Chemical Biology Laboratory, Center for Cancer Research, National Cancer Institute, Frederick, MD, USA

Correspondence
Stephen H. Hughes, HIV Dynamics and Replication Program, Center for Cancer Research, National Cancer Institute, Frederick, MD 21702, USA.
Email: hughesst@mail.nih.gov

Abstract

Non-nucleoside reverse transcriptase inhibitors (NNRTIs) inhibit reverse transcription and block the replication of HIV-1. Currently, NNRTIs are usually used as part of a three-drug combination given to patients as antiretroviral therapy. These combinations involve other classes of anti-HIV-1 drugs, commonly nucleoside reverse transcriptase inhibitors (NRTIs). However, attempts are being made to develop two-drug maintenance therapies, some of which involve an NNRTI and an integrase strand transfer inhibitor. This has led to a renewed interest in developing novel NNRTIs, with a major emphasis on designing compounds that can effectively inhibit the known NNRTI-resistant mutants. We have generated and tested novel rilpivirine (RPV) analogs. The new compounds were designed to exploit a small opening in the upper right periphery of the NNRTI-binding pocket. The best of the new compounds, **12**, was a more potent inhibitor of the NNRTI-resistant mutants we tested than either doravirine or efavirenz but was inferior to RPV. We describe the limitations on the modifications that can be appended to the "upper right side" of the RPV core and the effects of substituting other cores for the central pyrimidine core of RPV and make suggestions about how this information can be used in NNRTI design.

KEYWORDS

binding pocket, drug resistance, HIV, inhibitor, reverse transcriptase

1 | INTRODUCTION

Although the available anti-HIV drugs can, in combination, block viral replication, current therapies do not eliminate the viral infection. As a consequence, patients are currently prescribed multiple drugs (usually three). This approach is called combination antiretroviral therapy (cART). cART is the standard of care because treating patients with monotherapies fails to completely suppress HIV-1 replication, which leads to the rapid emergence of drug resistance (Havlir, McLaughlin, & Richman, 1995; Shafer et al., 2003). In most patients who are compliant, there is a decrease, over several months, in the level of viral RNA in the blood to levels below what can be detected in standard commercial assays (Maldarelli et al., 2007; Perelson et al., 1997). The most effective anti-HIV therapies target the HIV-1 viral enzymes protease, reverse transcriptase (RT), and integrase. The current standard of care for treatment-naïve patients includes an integrase strand transfer inhibitor (INSTI) plus two additional nucleoside reverse transcriptase inhibitors

(NRTIs), for example, bictegravir/tenofovir alafenamide/emtricitabine, dolutegravir/abacavir/lamivudine, or dolutegravir/tenofovir/emtricitabine (U.S. Department of Health and Human Service, 2019, G-4). However, there are clinical situations (including some types of salvage therapies) in which the cART regimen includes a non-nucleoside reverse transcriptase inhibitor (NNRTI; U.S. Department of Health and Human Service, 2019, G-1). There are six FDA-approved NNRTIs; a seventh, elsulfavirine, is approved for use only in Russia (Al-Salama, 2017). Only three of the approved NNRTIs, rilpivirine (RPV), doravirine (DOR), and efavirenz (EFV), are currently recommended for use in combination therapies (Figure 1; U.S. Department of Health and Human Service, 2019, G-1); the other three approved NNRTIs, nevirapine (NVP), delavirdine, and etravirine, are either sparingly recommended or have been discontinued (Gathe et al., 2011; Namasivayam et al., 2019; Scott & Perry, 2000; Wang, De Clercq, & Li, 2019). In low- to middle-income countries, EFV plus two NRTIs or NVP plus two NRTIs are still recommended treatment strategies. Attempts are being made to develop long-acting cART formulations and two-drug maintenance therapies for those who are fully suppressed. As is discussed in more detail below, some of the long-acting therapies, and some of the two-drug maintenance therapies that are being tested, include NNRTIs. Having additional NNRTIs that are broadly effective against the known drug-resistant mutants would be quite helpful.

NNRTIs bind in a largely hydrophobic pocket about 10 Å from the polymerase active site of RT (Das & Arnold, 2013a, 2013b). The binding of an NNRTI causes a conformational change that moves the end of the viral DNA away from the polymerase active site, blocking DNA synthesis (Das, Martinez, Bauman, & Arnold, 2012; Sluis-Cremer & Tachedjian, 2008). Host DNA polymerases do not have a structure that is similar to the NNRTI-binding site (Das, Lewi, Hughes, & Arnold, 2005), and in general, NNRTIs have little or no toxicity for the host (Margolis, Heverling, Pham, & Stolbach, 2014). However, the NNRTI-binding site of HIV RT is not evolutionarily well conserved (Ren et al., 2002; Tebit et al., 2010), and the emergence of resistance to NNRTIs is well documented (Wensing et al., 2019; Xavier Ruiz & Arnold, 2020).

There is an increased interest in developing drugs, and combination therapies, that can be used in long-acting formulations, both for antiviral therapy in those who are already infected and for preventive strategies (pre-exposure prophylaxis; PrEP; Cohen, 2018; Gulick & Flexner, 2019; Mayer et al., 2015; McCormack et al., 2016). Some of the long-acting therapies that are currently under development or in late-phase clinical trials are based on combinations of NNRTIs and INSTIs (Gulick, 2018; Margolis et al., 2015, 2017). In addition, there have been trials to test whether it is possible, in fully suppressed patients, to switch to a two-drug regimen for the maintenance of viral suppression. Some of the maintenance regimens being tested comprise an NNRTI and an INSTI, for example dolutegravir (DTG) and RPV, DTG and lamivudine (3TC), or boosted darunavir and RPV (Cahn et al., 2019; Casado, Monsalvo, Rojo, Fontecha, & Rodriguez-Sagrado, 2018; Llibre et al., 2018; Pasquau et al., 2019). These simplified maintenance therapies, if successful, would reduce both the cost of the therapy and the exposure to drugs over a lifetime of therapy (Dowers, Zamora, Barakat, & Ogbuagu, 2018; Llibre et al., 2018).

Although all NNRTIs bind in the same hydrophobic pocket of RT, there is no single consistent chemical structure or theme that defines what constitutes a successful NNRTI (Gu, Lu, Liu, Ju, & Zhu, 2018); however, the most recently FDA-approved NNRTIs, RPV and DOR, have a central core, with two appended aromatic rings. The structures of RPV and DOR differ significantly, and the two compounds bind differently within the NNRTI-binding pocket (Das et al., 2008; Feng et al., 2015; Smith, Pauly, Akram, Melody, Ambrose, et al., 2016). As might be expected, the compounds differ in terms of their ability to retain potency against the known NNRTI-resistant mutants (Smith, Pauly, Akram, Melody, Ambrose, et al., 2016).

Recently, we developed a series of RPV analogs that displayed potent antiviral activities not only against WT HIV-1, but also against many of the well-characterized NNRTI-resistant mutants, including DOR-resistant mutants (Smith, Pauly, Akram, Melody, Rai, et al., 2016). The new RPV analogs have various functional groups added to the central pyrimidine ring of RPV, and in some of the analogs, the central pyrimidine ring was replaced with either a 2,6-substituted purine ring system or a 2,9-substituted purine

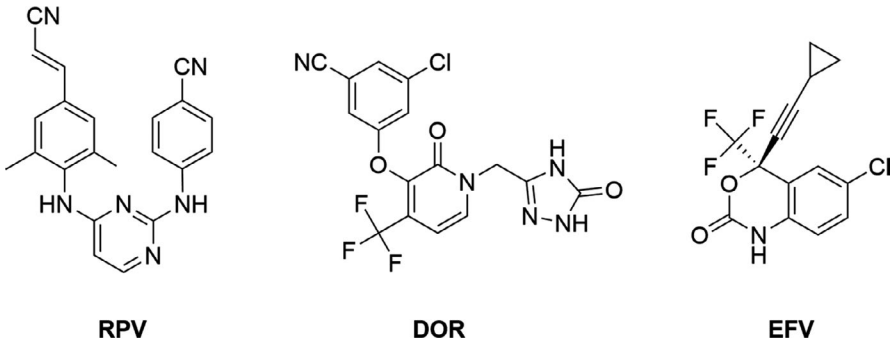

FIGURE 1 Chemical structures of the NNRTIs used in cART. The chemical structures of the FDA-approved NNRTIs RPV, DOR, and EFV are shown

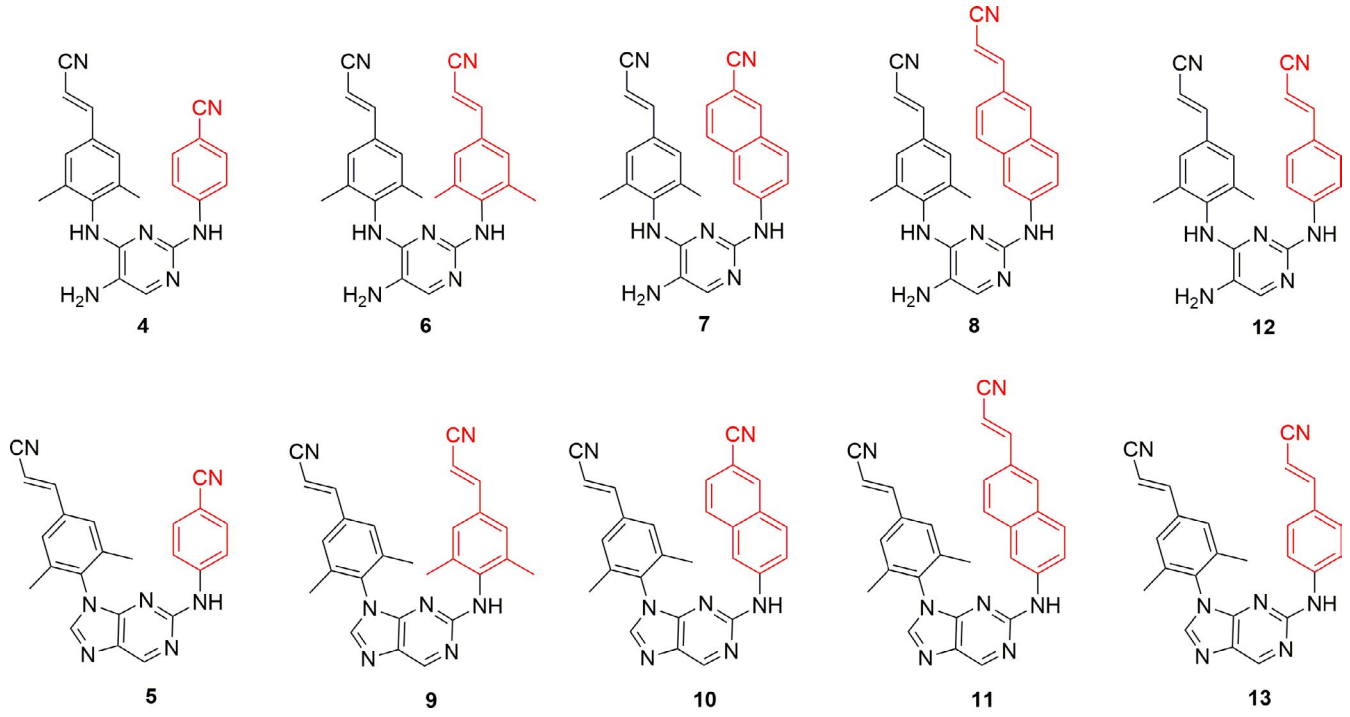

FIGURE 2 Chemical structures of the new RPV analogs. The structures of the lead compounds **4** and **5** and the new compounds used in this study are shown with the modifications appended to the aromatic ring on the right side of pyrimidine core depicted in red [Colour figure can be viewed at wileyonlinelibrary.com]

system. We also made modifications to the appended aromatic ring on the right side of RPV (depicted in red as shown in Figure 2), which is, in RPV, a benzonitrile. In the initial experiments, most of the modifications we tested were small (Johnson et al., 2012). In the experiments we report here, we chose two of the most promising compounds as leads and used them to extend our exploration of RPV modifications (Johnson et al., 2012; Smith, Pauly, Akram, Melody, Rai, et al., 2016). We generated compounds with novel modifications to the right side of the lead compounds and tested whether the new compounds could potently inhibit both WT HIV-1 and a panel of well-characterized NNRTI-, DOR- and RT-resistant mutants, some of which have mutations outside the NNRTI-binding pocket. One compound, **12**, was more broadly potent than DOR and was slightly better than EFV; however, none of the new compounds were better than the lead compounds. We discuss why the new compounds were not as effective as the leads from which they were derived and describe how the new data can be used to help guide the design of additional derivatives.

2 | METHODS AND MATERIALS

2.1 | NNRTI synthesis

EFV was purchased from Sigma. The acquisitions of RPV and DOR have been discussed previously (Smith, Pauly, Akram, Melody, Ambrose, et al., 2016; Smith, Pauly, Akram, Melody, Rai, et al., 2016). The synthesis of RPV analogs **4** and **5** has been described. Compound **4** was previously reported as compound **7**, and compound **5** was previously reported as compound **27** (Johnson et al., 2012). The synthesis and characterization of RPV analogs **6**, **7**, **8**, **9**, **10**, **11**, **12**, and **13** are described as follows. The arylamines used in the synthesis of these compounds are shown in Scheme 1, A. Ar_1 was synthesized from 4-bromo-2,6-dimethyl-aniline and acrylonitrile by a Heck coupling method (Schils et al., 2008). That paper also describes a workup, which combines solvent Michael addition to the *Z*-isomer and selective crystallization of the *E*-isomer to give greater than 98% enrichment of the *E*-isomer as determined by NMR. Ar_2 and Ar_4 were synthesized by adapting the Shils et.al. procedure (Schils et al., 2008) to 4-bromoaniline and 6-bromonaphthalen-2-amine, respectively. Ar_2 required two rounds of Michael addition–recrystallization to give greater than 95% *E*-isomer as determined by NMR. Ar_4 was not enriched by that procedure but was enriched to greater than 95% *E*-isomer by three rounds of sequential recrystallization from methanol. Ar_3 was synthesized by treating 6-bromonaphthalen-2-amine with copper (I) cyanide in DMF at 160°C.

The remaining analogs were synthesized using similar procedures as outlined in Scheme 1, B. Commercially available 2,4-dichloro-5-nitropyrimidine was reacted with (E)-3-(4-amino-3,5-dimethylphenyl)acrylonitrile (Ar_1) in a neat reaction at 140°C giving the 4-substituted pyrimidine along with a

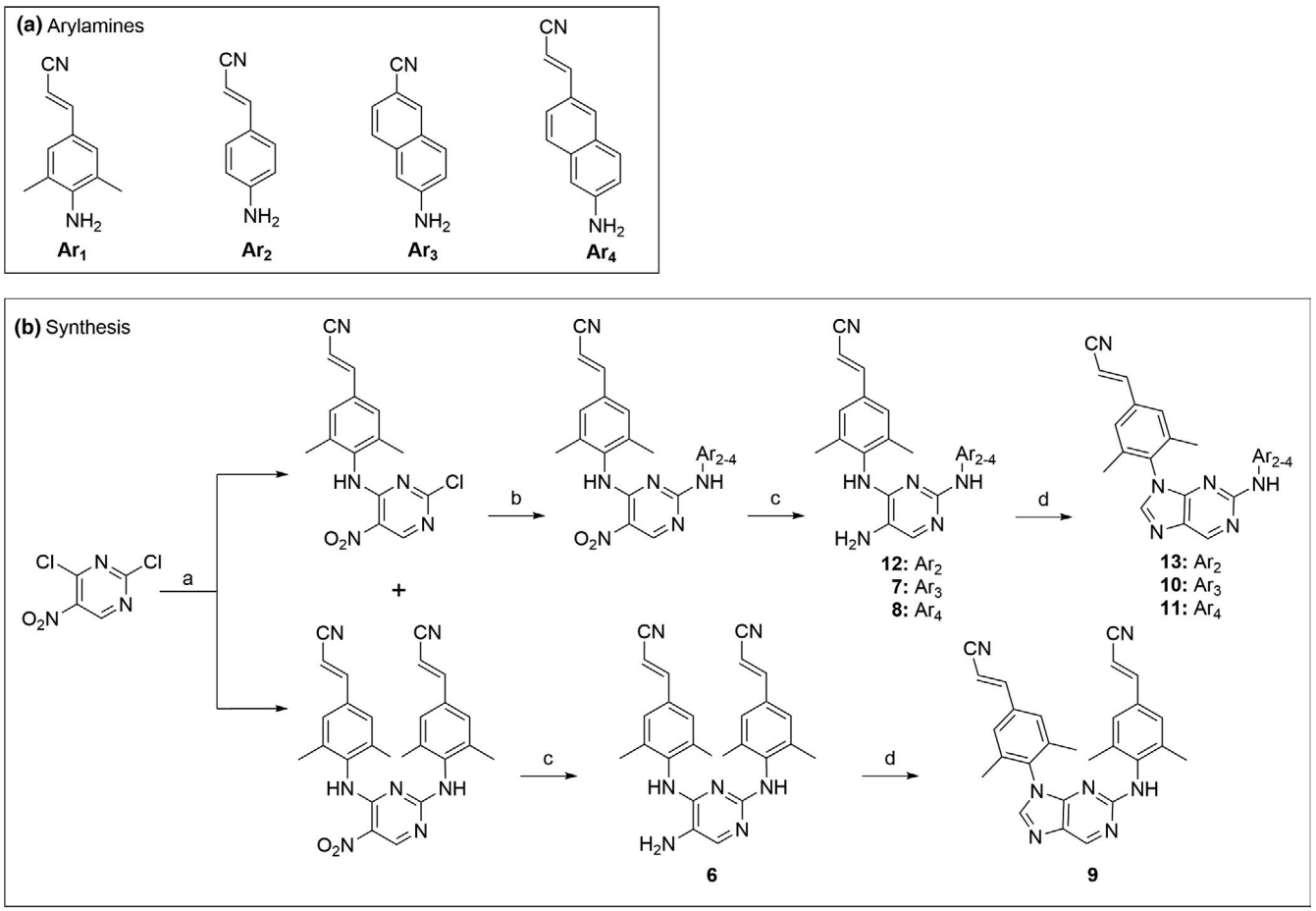

SCHEME 1 (a) The structures of the four arylamines used in the synthesis of compounds. (b) The synthetic process used to give the analogs used in this study

lesser amount of the 2,4-disubstituted pyrimidine, which would later give analogs **6** and **9**. The 4-substituted pyrimidines were substituted at the 2-chloro position with the remaining anilines $Ar_{2\text{-}4}$ by microwave heating at 110°C in DMF. The 5-nitro group was reduced with stannous chloride in ethanol at 60°C to give the five 2,4-arylamino-5-aminopyridines **6**,**7**, **8**, and **12**. The purine ring was formed by treating these analogs with triethyl orthoformate (neat) at 100°C to give purine compounds **9**, **10**, **11**, and **13**. All analogs were purified by preparative scale reverse-phase HPLC using acetonitrile–water gradients containing 0.1% trifluoroacetic acid. Product peaks were frozen and lyophilized to give amorphous solids.

NMR spectra were recorded on a Bruker spectrometer. The following abbreviations were used to describe peak patterns: s = singlet, d = doublet, dd = doublet of doublets, t = triplet, and m = multiplet. Low-resolution, positive-ion MS analyses (LC/MS) were carried out on an Agilent LC/MSD single quadrupole system, equipped with an in-line diode-array UV detector, to assess compound identity and homogeneity. Samples were analyzed by LC/MS using a narrow-bore (100 × 2.1 mm), small-particle (3.5 μm), Zorbax Rapid-Resolution reversed-phase C18 column coupled with a C18 guard column (12.5 × 2.1 mm) eluted with a 5%–90% gradient of methanol/water containing 0.1% acetic acid at a flow rate of 300 μl/min for separations. Samples were analyzed using atmospheric pressure chemical ionization (APCI). The UV chromatograms at 270 nm were used to assess purity, which was greater than 95% for all compounds.

2.1.1 | 6: (2E,2′E)-3,3′-(((5-aminopyrimidine-2,4-diyl)bis(azanediyl))bis(3,5-dimethyl-4,1-phenylene))diacrylonitrile

^{1}H NMR (400 MHz, DMSO-d_6) δ 9.58 (s, 1H), 9.48 (s, 1H), 7.56 (dd, J = 16.7, 1.6 Hz, 2H), 7.39 (d, J = 10.3 Hz, 4H), 7.16 (s, 1H), 6.41 (dd, J = 16.7, 1.8 Hz, 2H), 2.13 (s, 6H), 2.05 (s, 6H).

^{13}C NMR (100 MHz, DMSO-d_6) δ 158.35, 158.02, 157.69, 155.91, 149.95, 149.92, 148.67, 136.98, 136.91, 136.07, 135.51, 132.86, 132.69, 127.65, 127.30, 121.41, 118.78, 118.73, 96.95, 96.84,17.90, 17.72, 17.61.

MS (APCI) m/z = 436.2 $[M + H]^+$.

2.1.2 | 7: (E)-6-((5-amino-4-((4-(2-cyanovinyl)-2,6-dimethylphenyl)amino) pyrimidin-2-yl)amino)-2-naphthonitrile

^{1}H NMR (400 MHz, DMSO-d_6) δ 10.49 (s, 1H), 9.65 (s, 1H), 8.36 (d, J = 1.6 Hz, 1H), 7.84–7.72 (m, 3H), 7.62 (s, 2H), 7.56 (s, 1H), 7.48 (dd, J = 8.5, 1.7 Hz, 1H), 7.39 (dd, J = 9.0, 2.2 Hz, 1H), 7.13 (d, J = 8.6 Hz, 1H), 6.58 (d, J = 16.7 Hz, 1H), 2.21 (s, 6H).

2.1.3 | 8: (E)-3-(4-((5-amino-2-((6-((E)-2-cyanovinyl)naphthalen-2-yl)amino)pyrimidin-4-yl)amino)-3,5-dimethylphenyl)acrylonitrile

^{1}H NMR (400 MHz, DMSO-d_6) δ 10.54 (s, 1H), 9.81 (s, 1H), 7.97 (s, 1H), 7.77–7.66 (m, 4H), 7.62 (s, 2H), 7.58 (dd, J = 8.7, 1.8 Hz, 1H), 7.52 (s, 1H), 7.31 (dd, J = 8.9, 2.2 Hz, 1H), 7.13 (d, J = 8.8 Hz, 1H), 6.56 (d, J = 16.7 Hz, 1H), 6.41 (d, J = 16.6 Hz, 1H), 2.21 (s, 6H).

^{13}C NMR (100 MHz, DMSO-d_6) δ 159.05, 158.70, 155.42, 150.49, 149.94, 146.78, 137.50, 137.46, 136.43, 134.53, 133.11, 129.77, 129.28, 129.01, 128.65, 127.95, 127.64, 123.48, 120.71, 118.97, 118.87, 117.59, 114.67, 113.79, 97.27, 95.79, 17.95.

MS (APCI) m/z = 458.2 $[M + H]^+$.

2.1.4 | 9: (E)-3-(4-((9-(4-((E)-2-cyanovinyl)-2,6-dimethylphenyl)-9H-purin-2-yl)amino)-3,5-dimethylphenyl)acrylonitrile

^{1}H NMR (400 MHz, DMSO-d_6) δ 8.91 (s, 1H), 8.77 (s, 1H), 8.26 (s, 1H), 7.69–7.45 (m, 5H), 7.33 (s, 2H), 6.50 (d, J = 16.7 Hz, 1H), 6.31 (d, J = 16.7 Hz, 1H), 2.11 (s, 6H), 1.99 (s, 6H).

^{13}C NMR (100 MHz, DMSO d_6-) δ 158.43, 153.27, 150.32, 149.53, 149.29, 143.07, 139.88, 136.78, 136.28, 134.63, 134.51, 131.06, 127.62, 127.25, 127.04, 119.01, 118.57, 98.21, 95.58, 18.31, 17.53.

MS (APCI) m/z = 446.2 $[M + H]^+$.

^{13}C NMR (100 MHz, DMSO d_6-) δ 159.85, 159.53, 155.38, 150.47, 147.81, 139.76, 138.30, 136.98, 135.59, 134.21, 133.46, 129.58, 128.69, 128.15, 128.11, 126.98, 121.86, 119.84, 119.33, 115.70, 113.15, 106.30, 97.66, 18.57, 18.44.

MS (APCI) m/z = 432.2 $[M + H]^+$.

2.1.5 | 10: (E)-6-((9-(4-(2-cyanovinyl)-2,6-dimethylphenyl)-9H-purin-2-yl)amino)-2-naphthonitrile

^{1}H NMR (400 MHz, DMSO-d_6) δ 10.29 (d, J = 7.7 Hz, 1H), 9.11 (s, 1H), 8.64–8.54 (m, 1H), 8.49 (s, 1H), 8.37 (d, J = 1.5 Hz, 1H), 7.91 (d, J = 9.0 Hz, 1H), 7.83 (dd, J = 9.0, 2.2 Hz, 1H), 7.79–7.61 (m, 5H), 6.61 (d, J = 16.7 Hz, 1H), 2.05 (s, 6H).

^{13}C NMR (100 MHz, DMSO-d_6) δ 156.34, 152.49, 149.59, 149.37, 144.20, 141.50, 136.92, 135.57, 134.86, 134.38, 133.76, 128.85, 128.10, 127.88, 127.66, 127.35, 126.73, 121.70, 119.59, 118.62, 112.09, 105.21, 98.41, 17.66, 17.55.

MS (APCI) m/z = 442.1 $[M + H]^+$.

2.1.6 | 11: (E)-3-(6-((9-(4-((E)-2-cyanovinyl)-2,6-dimethylphenyl)-9H-purin-2-yl)amino) naphthalen-2-yl)acrylonitrile

^{1}H NMR (400 MHz, DMSO-d_6) δ 10.16 (s, 1H), 9.09 (s, 1H), 8.53–8.49 (m, 1H), 8.47 (s, 1H), 7.99 (s, 1H), 7.82–7.67 (m, 7H), 7.57 (d, J = 8.7 Hz, 1H), 6.61 (d, J = 16.7 Hz, 1H), 6.48 (d, J = 16.6 Hz, 1H), 2.06 (s, 6H).

^{13}C NMR (100 MHz, DMSO-d_6) δ 158.45, 156.51, 152.53, 150.69, 149.61, 149.35, 144.01, 140.24, 136.91, 135.09, 134.82, 134.43, 129.48, 129.07, 128.98, 128.04, 127.90, 127.65, 127.48, 123.37, 121.04, 119.23, 118.63, 112.51, 98.37, 95.15, 17.56.

MS (APCI) m/z = 468.2 $[M + H]^+$.

2.1.7 | 12: (E)-3-(4-((5-amino-2-((4-((E)-2-cyanovinyl)phenyl)amino)pyrimidin-4-yl) amino)-3,5-dimethylphenyl)acrylonitrile

^{1}H NMR (400 MHz, DMSO-d_6) δ 10.38 (s, 1H), 9.80 (s, 1H), 7.70 (d, J = 16.7 Hz, 1H), 7.56–7.44 (m, 4H), 7.29–7.12 (m, 4H), 6.53 (d, J = 16.7 Hz, 1H), 6.16 (d, J = 16.7 Hz, 1H), 2.17 (s, 6H).

^{13}C NMR (100 MHz, DMSO-d_6) δ 158.95, 158.60, 155.25, 150.08, 149.83, 140.89, 137.55, 136.30, 132.99, 128.23, 127.83, 127.50, 119.04, 118.84, 118.60, 97.07, 94.12, 17.90.

MS (APCI) m/z = 408.2 $[M + H]^+$.

2.1.8 | 13: (E)-3-(4-((9-(4-((E)-2-cyanovinyl)-2,6-dimethylphenyl)-9H-purin-2-yl)amino) phenyl)acrylonitrile

^{1}H NMR (400 MHz, DMSO-d_6) δ 10.08 (s, 1H), 9.04 (s, 1H), 8.42 (s, 1H), 7.83–7.76 (m, 2H), 7.72–7.67 (m, 1H), 7.63 (s, 2H), 7.55–7.44 (m, 3H), 6.58 (d, J = 16.7 Hz, 1H), 6.22 (d, J = 16.6 Hz, 1H), 2.01 (s, 6H).

^{13}C NMR (100 MHz, DMSO-d_6) δ 156.25, 152.53, 150.22, 149.60, 149.31, 144.15, 143.55, 136.87, 134.79, 134.34, 134.34, 128.55, 128.01, 127.65, 126.40, 119.43, 118.59, 117.77, 98.37, 92.84, 17.51.

MS (APCI) m/z = 418.1 $[M + H]^+$.

2.2 | Cell-based assays

HIV-based viral vectors with either a WT or a mutant RT were used in single-round infectivity assays to determine the antiviral potencies (half maximal effective concentration, EC_{50} values) of the compounds, and the cellular cytotoxicities were measured using an ATP-dependent luminescence assay as previously described (Smith & Hughes, 2014). A modified version of the single-round infectivity assay was used to determine the replication capacity of the NNRTI-resistant mutant vectors. Briefly, 200 ng of a WT or NNRTI-resistant mutant HIV-1 based vector was added to 96-well plates, incubated for 48 hr, and luciferase activity was measured. The luciferase activity of the WT virions was set to 100%, from which the infectivity of the mutant virions was measured as a percentage of WT activity.

2.3 | Vector constructs

The vector pNLNgoMIVR-ΔENV.LUC has been described previously (Smith, Zhao, Burke, & Hughes, 2018). The NNRTI-resistant mutants used in this study have been described previously (Smith, Pauly, Akram, Melody, Ambrose, et al., 2016; Smith, Pauly, Akram, Melody, Rai, et al., 2016).

2.4 | Computer modeling

All modeling was conducted using MOE 2019.01 02 (Chemical Computing Group). RPV in the RT NNRTI-binding pocket (PDB ID: 2ZD1; Das et al., 2008) was used as a structural template to dock compounds **7**, **12**, and **13** into the binding pocket. The docking placement methodology triangle matcher was initially scored by London dG. Rigid receptor was used for the postrefinement, and the final scoring methodology was GBVI/WSA dG.

3 | RESULTS

3.1 | Design of new RPV analogs

In previous studies, we showed that the RPV analogs **4** (previously reported as compound **7**) and **5** (previously described as compound **27**) were able to potently inhibit both WT HIV-1 and several NNRTI-resistant mutants (Johnson et al., 2012; Smith, Pauly, Akram, Melody, Rai, et al., 2016). Published structural studies have described a small hydrophobic pocket formed by residues P225, F227, and L234 that resides in the upper right region of the NNRTI-binding pocket (Figure 3; Das et al., 2008, 2012). We prepared a series of new compounds, using compounds **4** and **5** as leads, which have modifications to the right side aromatic ring (Figure 2; shown in red). We designed the new compounds to have modifications that could interact with the small hydrophobic pocket formed by residues P225, F227, and L234. Compounds **6**, **7**, **8**, and **12** are derivatives of **4** and contain, on the right side, appended to a benzene ring, cyanonaphthalene (**7**), naphthalene-2-acrylonitrile (**8**), or acrylonitrile (**12**). Compound **6** has a cyanoethenyl appended to a dimethylbenzene ring. Compounds **9** (cyanoethenyl), **10** (cyanonaphthalene), **11** (naphthalene-2-acrylonitrile), and **13** (acrylonitrile) are derivatives of **5** and have the same series of modified aromatic rings on the right side, but the central core is a 2,9-substituted purine rather than a pyrimidine.

3.2 | Comparing the cytotoxicities and antiviral potencies against WT HIV-1 of the new RPV analogs and the FDA-approved NNRTIs

To determine the potency of the new compounds, we tested their abilities to inhibit WT HIV-1 in a single-round infection assay (Table 1). Compounds **7** (2.3 ± 0.3 nM), **10** (2.3 ± 0.2 nM), **12** (1.2 ± 0.2 nM), and **13** (1.4 ± 0.2 nM) all potently inhibited WT HIV-1, with EC_{50} values less than 2.5 nM. In comparison, RPV and DOR, and the lead compounds **4** and **5**, have been previously shown to inhibit WT HIV-1 with subnanomolar potencies (Johnson et al., 2012; Smith, Pauly, Akram, Melody, Rai, et al., 2016). We also measured the antiviral activity of EFV against WT HIV-1; it potently inhibited WT HIV-1 with an EC_{50} of 0.9 ± 0.1 nM. Some of the new compounds, **6**, **8**, **9**, and **11** were less potent, in terms of their ability to inhibit WT HIV-1 (Table 1). The cytotoxicities of the new compounds and EFV were determined and compared with RPV, DOR, and the lead compounds **4** and **5** (Table 1). In general, NNRTIs have few problems with cytotoxicity when compared to the other major class of RT inhibitors, NRTIs. Among the FDA-approved NNRTIs, DOR was the best in terms of low cytotoxicity (180.6 ± 3.5 μM), while RPV is more toxic (20.6 ± 1.5 μM), and EFV (36.4 ± 1.6 μM) had a CC_{50} that was similar to RPV. Of the new compounds, **9** (191.6 ± 11.0 μM) and **13** (>250 μM) had favorable cytotoxicities; however, the cytotoxicities of remaining compounds ranged from a CC_{50} value of 10.8 μM (both **8** and **10**) to 44.9 μM (**6**). Both **12** and **13** had therapeutic indexes of >25,000, which is similar to the FDA-approved NNRTIs and the lead compounds, **4** and **5**. This initial screening of the new compounds suggests that these are the compounds that have the greatest potential.

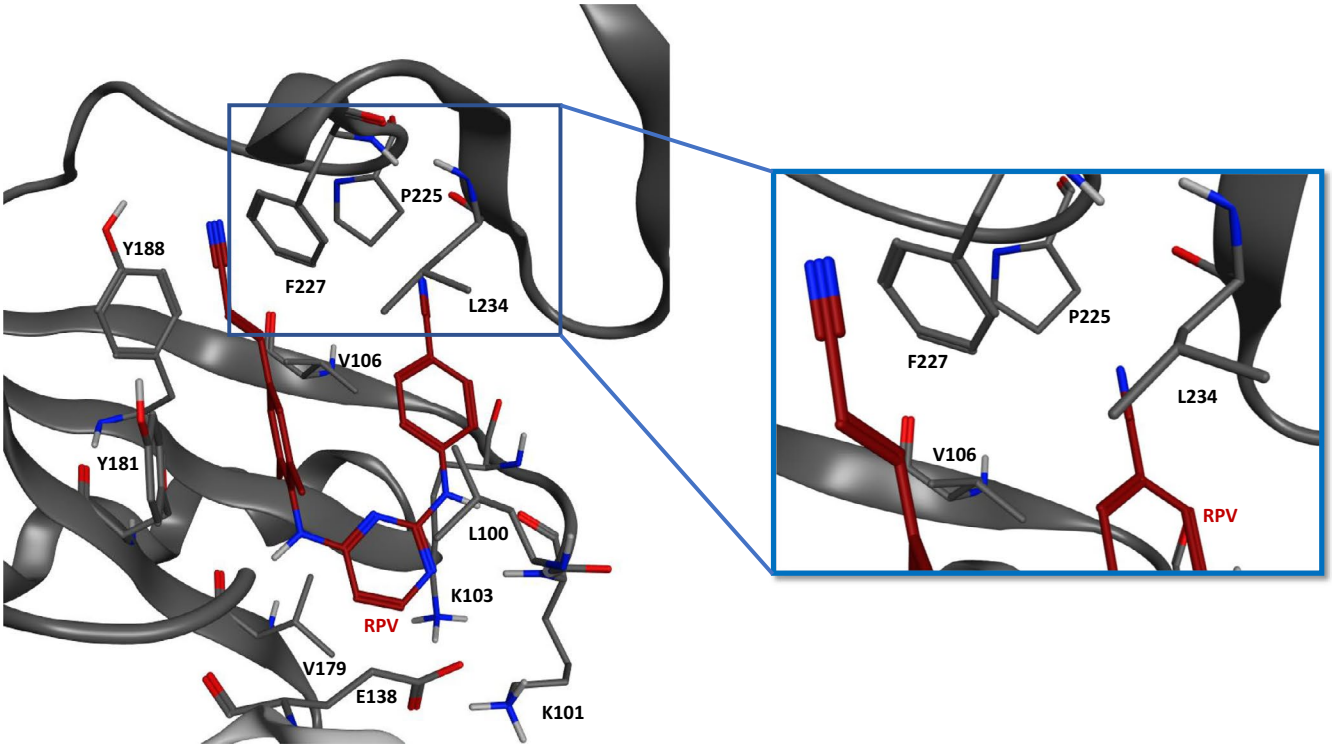

FIGURE 3 The small hydrophobic pocket formed by residues P225, F227, and L234 in the upper right periphery of the NNRTI-binding pocket. A structure of RPV (maroon) in the NNRTI-binding pocket is shown with the residues that comprise the binding pocket labeled in black. This small hydrophobic pocket is the place where the modifications on the upper right of the new RPV analogs are designed to bind; this small pocket is outlined by a blue square. The right inset shows a close-up of the small hydrophobic pocket with the benzonitrile modification of RPV bound in it [Colour figure can be viewed at wileyonlinelibrary.com]

3.3 | Comparison of antiviral potencies of RPV analogs and FDA-approved NNRTIs against well-known NNRTI-resistant mutants

As mentioned above, NNRTIs are potent inhibitors of WT HIV-1; however, because the NNRTI-binding site primarily consists of hydrophobic residues that are not strongly conserved evolutionarily, resistant mutants can and do emerge against them (Wang et al., 2019; Wensing et al., 2019). Treatment with the first-generation NNRTIs saw the emergence of a number of resistance mutations, most of which were in or near the NNRTI-binding pocket. New NNRTIs have been developed that can effectively inhibit some of the NNRTI-resistant mutants that emerged against the first-generation NNRTIs; however, even the most advanced NNRTIs, like RPV and DOR, are susceptible to some mutants. We tested the efficacies of the new RPV analogs against the signature NNRTI-resistant mutants L100I, K103N, V106A, E138K, Y181C, Y188L, H221Y, and K103N/Y181C and then compared the efficacies of the new compounds to RPV, DOR, and EFV and the lead compounds **4** and **5** (Table 2; Figure S1). Of the new compounds, **12** was the most successful in terms of its ability to inhibit the NNRTI-resistant mutants we tested; compound **7** was the second best. The only mutants in the panel that caused a significant reduction in potency for **12** were Y188L (44.0 ± 2.6 nM) and the double mutant K103N/Y181C (22.4 ± 1.1 nM). The antiviral profile of **12** against this panel of NNRTI-resistant mutants was very similar to the lead compound **5**; importantly, **12** was much more effective than the FDA-approved NNRTIs DOR and EFV. However, the antiviral profile of RPV analog **12** was inferior to both RPV and the lead compound, **4**.

Compound **7** also potently inhibited some of the NNRTI-resistant mutants, notably L100I (4.5 ± 0.4 nM), K103N (4.0 ± 0.8 nM), and H221Y (2.8 ± 0.2 nM). The NNRTI-resistant mutants V106A, E138K, and Y181C all caused small reductions in susceptibility to compound **7**, while NNRTI-resistant mutants Y188L (152.4 ± 21.3 nM) and K103N/Y181C (156.2 ± 12.7 nM) caused large reductions in susceptibility to **7** (Table 2). Both **10** and **13** retained high potencies against the NNRTI-resistant mutant H221Y, 3.4 ± 0.3 and 2.6 ± 0.7 nM, respectively; however, only **13** retained moderately potent efficacies against K103N and V106A, while a loss in potency was observed for **10** against K103N and V106A (Table 2). Compound **10** lost potency against L100I, E138K, Y181C, Y188L, and K103N/Y181C. Compound **13** lost potency against L100I, E138K, Y181C, Y188L, and K103N/Y181C (Table 2). Compounds **6**, **8**, **9**, and **11** were largely ineffective against the NNRTI-resistant mutants in this panel. Modeling the binding of the

TABLE 1 Cytotoxicities and antiviral potencies of the new RPV analogs and the FDA-approved NNRTIs against WT HIV-1

	CC_{50}	WT	TI
RPV	20.6 ± 1.5 μM	0.2 ± 0.1 nM	>25,000
DOR	180.6 ± 3.5 μM	0.7 ± 0.1 nM	>25,000
EFV	36.4 ± 1.6 μM	0.9 ± 0.1 nM	>25,000
4	51.1 ± 4.8 μM	0.5 ± 0.1 nM	>25,000
5	30.5 ± 3.9 μM	0.5 ± 0.1 nM	>25,000
6	44.9 ± 0.6 μM	27.2 ± 3.3 nM	1,651
7	23.0 ± 2.3 μM	2.3 ± 0.3 nM	10,000
8	10.8 ± 0.7 μM	6.8 ± 0.6 nM	1,588
9	191.6 ± 11.0 μM	10.4 ± 0.6 nM	18,423
10	10.8 ± 1.2 μM	2.3 ± 0.2 nM	4,696
11	17.1 ± 0.8 μM	10.2 ± 1.9 nM	1,676
12	32.2 ± 1.5 μM	1.2 ± 0.2 nM	>25,000
13	>250 μM	1.4 ± 0.2 nM	>25,000

Note: The CC_{50} values were determined for the approved NNRTIs and RPV analogs. The EC_{50} values for the approved NNRTIs and the new compounds were determined for WT HIV-1 in a single-round infection assay. The therapeutic indexes for the NNRTIs and RPV analogs were calculated. The error bars represent standard deviations of independent experiments, $n = 3$.

compounds using the previously solved structure of RPV bound to WT HIV RT, (Das et al. 2008) suggested that, for the compounds that failed, the modifications may have been too large to fit into the hydrophobic pocket formed by P225, F227, and L234 (data not shown). We confirmed that K103N (35.8 ± 9.1 nM), Y188L (76.8 ± 6.5 nM), and K103N/Y181C (36.0 ± 8.4 nM) all caused a significant loss in susceptibility to EFV; however, EFV was more broadly active against the NNRTI-resistant mutants in this panel than DOR. Based on these findings, we focused on the RPV analogs **7**, **10**, **12**, and **13**.

3.4 | Comparison of antiviral potencies of RPV analogs and FDA-approved NNRTIs against some other well-characterized NNRTI-resistant mutants

A number of NNRTI-resistant mutants have emerged against the first-generation FDA-approved NNRTIs, and we tested our new compounds against the lead compounds and the second-generation FDA-approved NNRTIs against some additional well-characterized NNRTI-resistant mutants K101P, Y181I, G190A, G190S, M230L, P236L, L100I/K103N, K101P/V179I, K103N/P225H, and V106A/G190A/F227L (Table 3; Figure S2). Of the four compounds we tested, **12** was the most broadly active against the second panel of NNRTI-resistant mutants. Compound **12** potently inhibited G190A, G190S, P236L, K103N/P225H, and V106A/

TABLE 2 Antiviral potencies of the new compounds and the FDA-approved NNRTIs against the NNRTI-resistant mutants

	WT	L100I	K103N	V106A	E138K	Y181C	Y188L	H221Y	K103N/Y181C
RPV	0.2 ± 0.1 nM	0.1 ± 0.03 nM	1.0 ± 0.2 nM	0.3 ± 0.1 nM	1.0 ± 0.1 nM	1.4 ± 0.4 nM	2.3 ± 0.2 nM	1.3 ± 0.1 nM	3.5 ± 0.3 nM
DOR	0.7 ± 0.1 nM	1.1 ± 0.2 nM	4.5 ± 2.8 nM	15.6 ± 4.0 nM	13.9 ± 2.4 nM	2.0 ± 0.2 nM	>100 nM	4.6 ± 1.8 nM	11.3 ± 5.9 nM
EFV	0.9 ± 0.1 nM	5.4 ± 0.9 nM	35.8 ± 9.1 nM	1.2 ± 0.2 nM	2.5 ± 0.4 nM	1.6 ± 0.1 nM	76.8 ± 6.5 nM	2.2 ± 0.4 nM	36.0 ± 8.4 nM
4	0.5 ± 0.1 nM	0.1 ± 0.03 nM	0.7 ± 0.1 nM	0.3 ± 0.03 nM	2.1 ± 0.1 nM	1.8 ± 0.2 nM	2.9 ± 0.2 nM	0.9 ± 0.1 nM	1.8 ± 0.1 nM
5	0.5 ± 0.1 nM	0.6 ± 0.02 nM	0.9 ± 0.2 nM	0.6 ± 0.1 nM	2.1 ± 0.1 nM	6.5 ± 0.2 nM	24.5 ± 4.0 nM	1.3 ± 0.4 nM	41.4 ± 3.6 nM
6	27.2 ± 3.3 nM	3,640 ± 437.1 nM	75.5 ± 5.6 nM	133.5 ± 9.7 nM	1.07 ± 0.06 μM	2.76 ± 0.58 μM	>5,000 nM	79.2 ± 6.4 nM	>5,000 nM
7	2.3 ± 0.3 nM	4.5 ± 0.4 nM	4.0 ± 0.8 nM	13.7 ± 3.4 nM	27.6 ± 2.4 nM	15.6 ± 2.0 nM	152.4 ± 21.3 nM	2.8 ± 0.2 nM	156.2 ± 12.7 nM
8	6.8 ± 0.6 nM	241.5 ± 35.4 nM	121.2 ± 9.7 nM	294.8 ± 29.0 nM	533.7 ± 27.1 nM	264.3 ± 15.9 nM	3,066.7 ± 916.6 nM	18.7 ± 2.5 nM	1,990 ± 425.8 nM
9	10.4 ± 0.6 nM	156.1 ± 30.6 nM	48.0 ± 4.2 nM	58.8 ± 6.0 nM	150.4 ± 6.9 nM	>5,000 nM	>5,000 nM	19.4 ± 2.2 nM	>5,000 nM
10	2.3 ± 0.2 nM	24.2 ± 6.1 nM	24.5 ± 4.9 nM	15.1 ± 1.0 nM	32.7 ± 4.4 nM	47.7 ± 7.8 nM	180.3 ± 14.7 nM	3.4 ± 0.3 nM	467.6 ± 88.8 nM
11	10.2 ± 1.9 nM	78.0 ± 11.7 nM	232.1 ± 22.3 nM	>5,000 nM	>5,000 nM	>5,000 nM	>5,000 nM	17.1 ± 2.1 nM	>5,000 nM
12	1.2 ± 0.2 nM	1.8 ± 0.2 nM	1.6 ± 0.2 nM	0.8 ± 0.2 nM	6.5 ± 0.9 nM	5.3 ± 0.8 nM	44.0 ± 2.6 nM	1.6 ± 0.1 nM	22.4 ± 1.1 nM
13	1.4 ± 0.2 nM	28.6 ± 7.6 nM	9.3 ± 0.7 nM	11.3 ± 2.2 nM	29.1 ± 1.9 nM	92.4 ± 10.0 nM	208.0 ± 12.0 nM	2.6 ± 0.7 nM	322.8 ± 56.7 nM

Note: Numerical values of the EC_{50} values and standard deviations ($n = 3$) of the FDA-approved NNRTIs and RPV analogs against the NNRTI-resistant single and double mutants are shown.

TABLE 3 Antiviral potencies of the new compounds and the FDA-approved NNRTIs against additional well-characterized NNRTI-resistant mutants

	WT	K101P	Y181I	G190A	G190S	M230L	P236L	L100I/K103N	K101P/V179I	K103N/P225H	V106A/G190A/F227L
RPV	0.2 ± 0.1 nM	6.2 ± 1.6 nM	8.8 ± 0.1 nM	0.4 ± 0.1 nM	0.1 ± 0.01 nM	1.7 ± 0.0 nM	0.2 ± 0.0 nM	2.3 ± 0.2 nM	93.5 ± 12.1 nM	0.6 ± 0.2 nM	0.5 ± 0.02 nM
DOR	0.7 ± 0.1 nM	1.0 ± 0.3 nM	0.6 ± 0.3 nM	1.2 ± 0.4 nM	4.6 ± 1.2 nM	51.1 ± 6.5 nM	2.0 ± 0.7 nM	2.0 ± 0.8 nM	1.5 ± 0.4 nM	25.3 ± 4.5 nM	>100 nM
EFV	0.9 ± 0.1 nM	112.3 ± 13.9 nM	0.9 ± 0.2 nM	1.1 ± 0.1 nM	17.1 ± 2.6 nM	14.3 ± 2.0 nM	0.2 ± 0.04 nM	488.5 ± 50.0 nM	35.1 ± 2.9 nM	50.4 ± 3.1 nM	184.8 ± 19.8 nM
4	0.5 ± 0.1 nM	9.0 ± 2.3 nM	19.0 ± 2.6 nM	0.3 ± 0.0 nM	0.4 ± 0.07 nM	4.0 ± 2.0 nM	0.2 ± 0.06 nM	1.7 ± 0.4 nM	81.4 ± 8.1 nM	1.1 ± 0.3 nM	1.4 ± 0.4 nM
5	0.5 ± 0.1 nM	4.9 ± 2.2 nM	23.1 ± 4.5 nM	0.2 ± 0.1 nM	0.1 ± 0.01 nM	4.2 ± 0.5 nM	0.2 ± 0.04 nM	39.8 ± 9.2 nM	16.6 ± 0.5 nM	2.1 ± 0.9 nM	2.2 ± 1.2 nM
7	2.3 ± 0.3 nM	98.7 ± 14.0 nM	757.7 ± 57.2 nM	1.4 ± 0.1 nM	1.0 ± 0.1 nM	21.4 ± 4.2 nM	1.2 ± 0.3 nM	264.6 ± 5.9 nM	308.4 ± 56.6 nM	25.3 ± 3.0 nM	5.2 ± 1.0 nM
10	2.3 ± 0.2 nM	65.9 ± 6.4 nM	1,637 ± 167.6 nM	1.6 ± 0.3 nM	2.1 ± 0.1 nM	33.8 ± 2.7 nM	1.6 ± 0.1 nM	385.8 ± 19.9 nM	96.9 ± 16.5 nM	103.3 ± 8.1 nM	7.0 ± 0.5 nM
12	1.2 ± 0.2 nM	126.3 ± 29.4 nM	255.1 ± 36.4 nM	0.7 ± 0.1 nM	0.2 ± 0.06 nM	16.9 ± 1.2 nM	0.6 ± 0.1 nM	16.1 ± 0.2 nM	270.5 ± 63.1 nM	1.6 ± 0.2 nM	2.5 ± 0.5 nM
13	1.4 ± 0.2 nM	280.3 ± 27.0 nM	3,088.7 ± 220.6 nM	0.9 ± 0.1 nM	1.2 ± 0.3 nM	60.0 ± 0.9 nM	1.1 ± 0.05 nM	252.1 ± 21.9 nM	551.6 ± 86.7 nM	29.1 ± 1.6 nM	4.7 ± 0.9 nM

Note: Numerical values of the EC_{50} values and standard deviations ($n = 3$) of the FDA-approved NNRTIs and the new compounds against the NNRTI-resistant single, double, and triple mutants are shown.

G190A/F227L with EC_{50} values that were similar to RPV and the lead compounds **4** and **5**. Compound **12** was more effective than both DOR and EFV against the NNRTI-resistant mutants K103N/P225H (1.6 ± 0.2 nM) and V106A/G190A/F227L (2.5 ± 0.5 nM). The EC_{50} values of DOR and EFV against K103N/P225H were 25.3 ± 4.5 and 50.4 ± 3.1 nM, respectively, and against V106A/G190A/F227L were >100 and 184.8 ± 19.8 nM, respectively. Compound **12** showed a moderate loss in potency against M230L and L100I/K103N (Table 3). The three NNRTI-resistant mutants K101P, V181I, and K101P/V179I, all of which have been previously shown to cause a loss of potency for RPV and the lead compounds **4** and **5**, also caused a large reduction in susceptibility to **12** (EC_{50} values > 100 nM). Although the potencies were lower for **12** against M230L (16.9 ± 1.2 nM) and L100I/K103N (16.1 ± 0.2 nM), these antiviral activities were better than DOR against M230L (51.1 ± 6.5 nM) and EFV against L100I/K103N (488.5 ± 50.0 nM). The other new compounds failed against a number of the NNRTI-resistant mutants in this panel. However, **7**, **10**, and **13** all potently inhibited G190A/S and P236L with EC_{50} values ≤ 2.1 nM. Overall, in terms of their ability to inhibit the mutants in this panel, RPV and the lead compounds **4** and **5** were more effective than **12**; however, **12** was a more broadly effective than EFV or DOR.

3.5 | Comparison of antiviral potencies of the new compounds and FDA-approved NNRTIs against DOR-resistant mutants

Because we are developing new RPV analogs and because we have previously demonstrated that RPV and DOR have non-overlapping resistance profiles that could potentially be exploited in combination therapy (Smith, Pauly, Akram, Melody, Ambrose, et al., 2016), we measured the ability of the RPV analogs to inhibit the DOR-resistant mutants V106A, L234I, V106A/F227, V106A/L234I, and V106A/F227L/L234I (Table 4; Figure S3). Compound **12** potently inhibited all of the DOR-resistant mutants with EC_{50} values <2.0 nM. These results are similar to the lead compounds **4** and **5** and similar to RPV, which inhibited all the DOR-resistant mutants with EC_{50} values ≤0.8 nM. Compounds **7**, **10**, and **13** all retained potency against L234I (EC_{50} values <2.3 nM); however, only **7** and **13** potently inhibited V106A/F227L/L234I (EC_{50} values <5.4 nM). The RT mutants V106A, V106A/F227L, and V106A/L234I all caused drops in susceptibility to **7**, **10**, and **13** (EC_{50} values ranging from >10 to <80 nM); V106A/F227/L234I caused a minor drop in susceptibility to **10** (13.1 ± 0.7 nM). Compared to EFV, using this panel of mutants, **12** had a slightly better antiviral profile. Out of the five DOR-resistant mutants, **12** was more potent against four of them (V106A, L234I, V106A/F227L, and V106A/F227/L234I).

TABLE 4 Antiviral potencies of the new compounds and FDA-approved NNRTIs against DOR-resistant mutants

	WT	V106A	L234I	V106A/F227L	V106A/L234I	V106A/F227L/L234I
RPV	0.2 ± 0.1 nM	0.3 ± 0.1 nM	0.1 ± 0.06 nM	0.8 ± 0.1 nM	0.1 ± 0.0 nM	0.2 ± 0.01 nM
DOR	0.7 ± 0.1 nM	15.6 ± 4.0 nM	6.8 ± 2.5 nM	>100 nM	>100 nM	>100 nM
EFV	0.9 ± 0.1 nM	1.2 ± 0.2 nM	0.8 ± 0.1 nM	4.9 ± 0.7 nM	0.3 ± 0.03 nM	3.4 ± 0.3 nM
4	0.5 ± 0.1 nM	0.3 ± 0.03 nM	0.2 ± 0.1 nM	1.3 ± 0.4 nM	0.3 ± 0.1 nM	0.4 ± 0.1 nM
5	0.5 ± 0.1 nM	0.6 ± 0.1 nM	0.1 ± 0.04 nM	2.9 ± 0.3 nM	0.4 ± 0.2 nM	0.7 ± 0.3 nM
7	2.3 ± 0.3 nM	13.7 ± 3.4 nM	1.1 ± 0.2 nM	18.7 ± 2.1 nM	25.7 ± 2.1 nM	3.5 ± 0.2 nM
10	2.3 ± 0.2 nM	15.1 ± 1.0 nM	2.3 ± 0.2 nM	28.1 ± 1.9 nM	79.1 ± 10.4 nM	13.1 ± 0.7 nM
12	1.2 ± 0.2 nM	0.8 ± 0.2 nM	0.5 ± 0.07 nM	2.0 ± 0.1 nM	1.4 ± 0.5 nM	1.3 ± 0.1 nM
13	1.4 ± 0.2 nM	11.3 ± 2.2 nM	1.8 ± 0.4 nM	11.2 ± 2.2 nM	36.6 ± 2.4 nM	5.4 ± 1.1 nM

Note: Numerical values of the EC_{50} values and standard deviations ($n = 3$) of the FDA-approved NNRTIs and the new compounds against the DOR-resistant single, double, and triple mutants are shown.

3.6 | Comparison of antiviral potencies of the new compounds and FDA-approved NNRTIs against mutants with resistance mutations located outside the NNRTI-binding pocket

We also compared our new compounds to RPV and the FDA-approved NNRTIs using a panel of RT-resistant mutants that have their resistance mutations located outside the NNRTI-binding pocket: E40K, D67E, K101E, V111A, M184I, M184V, K101E/M184I, K101E/M184V, E138K/M184I, and E138K/M184V (Table 5; Figure S4). Compound **12** potently inhibited almost all of the RT-resistant mutants (EC_{50} values ≤3.4 nM); there was a minor reduction in potency against E138K/M184I and E138K/M184V (Table 5). In comparison with RPV and the lead compounds **4** and **5**, the antiviral profile of **12** was nearly equivalent; however, there are some mutants for which **12** was slightly more potent than the FDA-approved NNRTIs. DOR failed to retain potency against D67E (46.0 ± 14.0 nM), while **12** potently inhibited this mutant (3.4 ± 0.5 nM). Against K101E, **12** had an EC_{50} value at 3.4 ± 0.5 nM while EFV lost potency (11.0 ± 1.2 nM). The remaining compounds **7**, **10**, and **13** all had similar, albeit weaker, antiviral profiles against the RT-resistant mutants when compared to **12**. These additional compounds effectively inhibited E40K, V111A, M184I, M184V, and K101E/M184V (EC_{50} values <5.0 nM); however, they lost potency against D67E, K101E/M184I, E138K/M184I, and E138K/M184V (EC_{50} values >7.0 nM).

3.7 | Modeling the binding of compound 12 using the structure of RPV in the NNRTI-binding pocket

Using the structure of RPV in the NNRTI-binding pocket as a template (PDB ID: 2ZD1; Figure 3; Das et al., 2008), we modeled the binding of compound **12** (Figure 4, panel a). As expected, the binding modes of the two NNRTIs are nearly identical. The difference in the two compounds (**12** has a cyanoethenylbenzyl modification instead of the benzonitrile that is present in RPV) was intended to allow the binding of the cyanoethenyl in the small hydrophobic pocket formed by residues P225, F227, and L234. This pocket is in the upper right of the NNRTI-binding pocket; according to the model, the cyanoethenyl moiety binds approximately 1.5 Å deeper into the pocket. Compound **7** was the second best of the new compounds in this study. Compound **7** was also based on lead compound **4** and has cyanonaphthalene constituent that, based on the models, binds approximately 1.3 Å deeper into the P225, F227, L234 hydrophobic pocket than RPV (Figure 4, panel b). In our models, the modifications to the RPV analogs **10** and **13**, which were built on lead **5**, do not bind in the small hydrophobic pocket (Figure 4, panel c). Their respective modifications interact with the back of the NNRTI-binding pocket between V106 and P236, which would explain their failure to retain potency against many of the NNRTI-resistant mutants (see Section 4).

4 | DISCUSSION

NNRTIs are well-established antiretrovirals that are currently used as one of the therapeutic options in cART. Recently, there has been an increased interest in using NNRTIs, particularly RPV, in combination with an INSTI, in long-acting formulations that are injected or implanted (Gulick & Flexner, 2019; Margolis et al., 2015, 2017). The initial results have been quite promising (Margolis et al., 2017), and it appears that this approach will be available as a therapeutic and/or preventative option in the near future. However, the emergence of drug-resistant strains of

TABLE 5 Antiviral potencies of the new compounds and FDA-approved NNRTIs against mutants with resistance mutations located outside the NNRTI-binding pocket

	WT	E40K	D67E	K101E	V111A	M184I	M184V	K101E/M184I	K101E/ M184V	E138K/M184I	E138K/M184V
RPV	0.2 ± 0.1 nM	0.3 ± 0.04 nM	0.8 ± 0.3 nM	2.6 ± 1.6 nM	0.3 ± 0.1 nM	0.2 ± 0.08 nM	0.1 ± 0.0 nM	0.7 ± 0.1 nM	0.2 ± 0.0 nM	1.1 ± 0.1 nM	1.3 ± 0.4 nM
DOR	0.7 ± 0.1 nM	1.5 ± 0.5 nM	46.0 ± 14.0 nM	0.4 ± 0.04 nM	0.3 ± 0.1 nM	0.6 ± 0.2 nM	0.7 ± 0.01 nM	2.3 ± 0.6 nM	0.2 ± 0.02 nM	1.4 ± 0.6 nM	3.0 ± 0.1 nM
EFV	0.9 ± 0.1 nM	0.3 ± 0.02 nM	3.7 ± 0.7 nM	11.0 ± 1.2 nM	0.2 ± 0.04 nM	0.2 ± 0.04 nM	0.3 ± 0.1 nM	0.9 ± 0.2 nM	1.5 ± 0.2 nM	2.2 ± 0.4 nM	2.1 ± 0.1 nM
4	0.5 ± 0.1 nM	0.5 ± 0.1 nM	4.5 ± 1.1 nM	2.3 ± 1.2 nM	0.2 ± 0.1 nM	0.12 ± 0.03 nM	0.4 ± 0.04 nM	1.3 ± 0.6 nM	0.7 ± 0.1 nM	2.9 ± 0.6 nM	2.4 ± 0.2 nM
5	0.5 ± 0.1 nM	0.5 ± 0.1 nM	1.1 ± 0.4 nM	1.2 ± 0.7 nM	0.1 ± 0.0 nM	0.2 ± 0.04 nM	0.2 ± 0.01 nM	0.5 ± 0.3 nM	0.9 ± 0.1 nM	0.9 ± 0.6 nM	1.8 ± 0.8 nM
7	2.3 ± 0.3 nM	1.9 ± 0.1 nM	9.7 ± 1.2 nM	9.9 ± 2.0 nM	0.2 ± 0.03 nM	1.6 ± 0.2 nM	2.0 ± 0.1 nM	9.4 ± 0.4 nM	3.0 ± 0.3 nM	23.0 ± 0.4 nM	20.6 ± 3.6 nM
10	2.3 ± 0.2 nM	4.2 ± 0.7 nM	10.0 ± 1.9 nM	13.4 ± 1.0 nM	0.4 ± 0.02 nM	1.3 ± 0.2 nM	3.1 ± 0.4 nM	14.0 ± 0.1 nM	4.7 ± 0.8 nM	16.9 ± 4.7 nM	32.3 ± 3.6 nM
12	1.2 ± 0.2 nM	0.8 ± 0.1 nM	3.4 ± 0.5 nM	3.4 ± 0.1 nM	0.1 ± 0.01 nM	0.4 ± 0.1 nM	1.1 ± 0.2 nM	3.1 ± 0.6 nM	1.9 ± 0.4 nM	6.1 ± 0.9 nM	6.8 ± 0.2 nM
13	1.4 ± 0.2 nM	1.7 ± 0.2 nM	9.5 ± 1.8 nM	9.7 ± 1.2 nM	0.2 ± 0.02 nM	0.5 ± 0.1 nM	2.2 ± 0.1 nM	7.0 ± 0.6 nM	3.9 ± 0.6 nM	19.5 ± 3.1 nM	21.6 ± 2.6 nM

Note: Numerical values of the EC_{50} values and standard deviations ($n = 3$) of the FDA-approved NNRTIs and the new compounds against the RT-resistant single and double mutants are shown.

HIV is a growing problem. Currently, in the Washington D.C. area, about twenty percent of new HIV-1 infections involve drug-resistant mutants (Gibson et al., 2019). Therefore, the development of new antiretrovirals is a necessity. However, although RPV is an effective inhibitor, like all other anti-HIV drugs, it selects for resistant strains of HIV. Thus, there is a need to develop new NNRTIs, particularly new compounds that will be broadly effective against the known NNRTI-resistant mutants. In an effort to seek improved solubility and bioavailability, others have reported the development of RPV analogs that have different modifications of the moieties that are linked to the pyrimidine core (Huang et al., 2019; Kang, Wang, et al., 2019; Kang, Zhang, et al., 2019; Liu et al., 2016). We have focused primarily on increasing the potency of RPV analogs against resistant strains of HIV.

Here, we tested new RPV analogs that were based on our previously described RPV analogs **4** and **5**. The goal was to make modifications on the right side of the two lead compounds. The modifications were intended to bind within a small hydrophobic pocket formed by residues P225, F227, and L234 located in the upper right periphery of the NNRTI-binding pocket. The idea was that the additional interactions between the modifications and the small binding pocket would increase the ability of the modified NNRTI(s) to bind to WT and mutant RTs.

RPV analog **12** was the best of the new RPV analogs and had an overall antiviral profile that was better than DOR and equivalent to, if not slightly better than, EFV. However, compound **12** was inferior to RPV and the lead compounds **4** and **5**. Against WT HIV-1 and the thirty-two NNRTI-resistant mutants used in this study, **12** had considerably better potencies against a total of twenty-nine out of thirty-two NNRTI-resistant mutants when compared to the other new RPV analogs we tested. Only compound **10** exhibited improved potencies against the NNRTI-resistant mutants K101P and K101P/V179I when compared to compound **12** (compound **7** also had a better potency against K101P when compared to **12**). Compound **12** had better potencies than EFV for seven out of the thirty-two NNRTI-resistant mutants, including six out of eight of the signature NNRTI-resistant mutants and three out of the four DOR-resistant mutants. When compared to DOR, **12** was more potent against nineteen of the thirty-two NNRTI-resistant mutants, including five of the eight signature NNRTI-resistant mutants, all of the DOR-resistant mutants, and six out of the ten other NNRTI-resistant mutants. However, when **12** was compared to RPV, using our panel of resistant mutants, it was generally less potent, although for twelve out of the thirty-two mutants, the EC_{50}s were nearly identical (within 1.0 nM), and for an additional twelve mutants, the EC_{50}s were within 6.0 nM.

In the experiments we report here, we developed RPV analogs that were designed to interact with a small hydrophobic

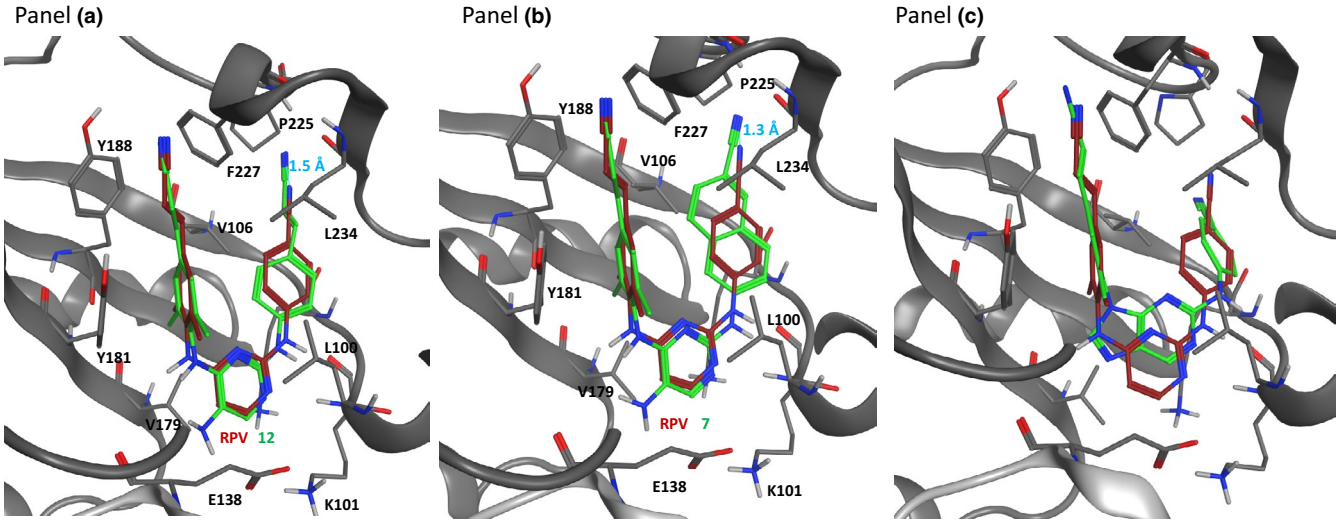

FIGURE 4 Modeling the binding of the RPV analog **12** to HIV-1 RT based on a structure of RPV in the NNRTI-binding pocket. Panel (a) shows a model of RPV analog **12** (green) docked into the structure of RPV (maroon) in the NNRTI-binding pocket. The distance between the acrylonitrile modification on to the benzene ring of **12** and the benzonitrile modification of RPV is shown in blue. The interactions between the acrylonitrile modification and the benzonitrile modification of RPV with the small hydrophobic pocket located in the upper right of the NNRTI-binding pocket are shown. Panel (b) shows a model of RPV analog **7** (green) docked into the structure of RPV (maroon) in the NNRTI-binding pocket. The distance between the cyanonaphthalene modification on the benzene ring of **7** and the benzonitrile modification of RPV is shown in blue with each of the modifications entering the small hydrophobic pocket in the upper right of the NNRTI-binding pocket. Panel (c) shows a model of RPV analog **13** (green) docked into the structure of RPV (maroon) in the NNRTI-binding pocket. The acrylonitrile modification of **13** interacts with the back of the NNRTI-binding pocket between V106 and P236 (not shown) and fails to enter the upper right of the NNRTI-binding pocket, which is also marked by a red circle. Residues in all panels that form the NNRTI-binding pocket are labeled in black [Colour figure can be viewed at wileyonlinelibrary.com]

patch in the upper right periphery of the NNRTI-binding pocket. Based on the results we obtained with the first set of derivatives, it does not appear that it will be easy to exploit this potential binding site. However, the derivatives that were made can be used to help to establish guidelines for the design and development of additional NNRTIs. The results suggest that the RPV analogs constructed using compound **4** as a lead compound were more effective than were the derivatives that were based on compound **5**. Thus, new NNRTI designs should focus on further optimization of a centralized core based on a pyrimidine ring, rather than using a purine as the core. Furthermore, the derivatives that we prepared in some cases reached (and in some cases appeared to exceed) the optimal length of the modifications that should be appended to the right hand ring, as defined by the acrylonitrile in compound **12**. Longer substituents appear to make the compounds vulnerable to mutations in the upper right periphery of the NNRTI-binding pocket. However, it should be possible, using a different centralized core, and/or different modifications, to create a new NNRTI that would be better able to broadly and effectively inhibit the known NNRTI-resistant mutants.

ACKNOWLEDGEMENTS

The authors would like to thank Teresa Burdette for help in preparing the manuscript. This research was supported by the Intramural Research Programs of the National Cancer Institute and the Intramural AIDS Targeted Antiviral Program.

CONFLICT OF INTEREST

The authors declare that they have no competing interests.

DATA AVAILABILITY STATEMENT

The datasets used and/or analyzed during the current study are available from the corresponding author on reasonable request.

ORCID

Stephen H. Hughes https://orcid.org/0000-0002-9176-4377

REFERENCES

Al-Salama, Z. T. (2017). Elsulfavirine: First global approval. *Drugs*, *77*(16), 1811–1816. https://doi.org/10.1007/s40265-017-0820-3

Cahn, P., Madero, J. S., Arribas, J. R., Antinori, A., Ortiz, R., Clarke, A. E., … Ustianowski, A. (2019). Dolutegravir plus lamivudine versus dolutegravir plus tenofovir disoproxil fumarate and emtricitabine in antiretroviral-naive adults with HIV-1 infection (GEMINI-1 and GEMINI-2): Week 48 results from two multicentre, double-blind, randomised, non-inferiority, phase 3 trials. *The Lancet*, *393*(10167), 143–155. https://doi.org/10.1016/S0140-6736(18)32462-0

Casado, J. L., Monsalvo, M., Rojo, A. M., Fontecha, M., & Rodriguez-Sagrado, M. A. (2018). Dolutegravir and rilpivirine for the maintenance treatment of virologically suppressed HIV-1 infection. *Expert Review of Clinical Pharmacology*, *11*(6), 561–570. https://doi.org/10.1080/17512433.2018.1478726

Cohen, J. (2018). Concern as HIV prevention strategy languishes. *Science*, *359*(6381), 1205. https://doi.org/10.1126/science.359.6381.1205

Das, K., & Arnold, E. (2013a). HIV-1 reverse transcriptase and antiviral drug resistance. Part 1. *Current Opinion in Virology*, *3*(2), 111–118. https://doi.org/10.1016/j.coviro.2013.03.012

Das, K., & Arnold, E. (2013b). HIV-1 reverse transcriptase and antiviral drug resistance. Part 2. *Current Opinion in Virology*, *3*(2), 119–128. https://doi.org/10.1016/j.coviro.2013.03.014

Das, K., Bauman, J. D., Clark, A. D. Jr, Frenkel, Y. V., Lewi, P. J., Shatkin, A. J., … Arnold, E. (2008). High-resolution structures of HIV-1 reverse transcriptase/TMC278 complexes: Strategic flexibility explains potency against resistance mutations. *Proceedings of the National Academy of Sciences USA*, *105*(5), 1466–1471. https://doi.org/10.1073/pnas.0711209105

Das, K., Lewi, P. J., Hughes, S. H., & Arnold, E. (2005). Crystallography and the design of anti-AIDS drugs: Conformational flexibility and positional adaptability are important in the design of non-nucleoside HIV-1 reverse transcriptase inhibitors. *Progress in Biophysics and Molecular Biology*, *88*(2), 209–231. https://doi.org/10.1016/j.pbiomolbio.2004.07.001

Das, K., Martinez, S. E., Bauman, J. D., & Arnold, E. (2012). HIV-1 reverse transcriptase complex with DNA and nevirapine reveals non-nucleoside inhibition mechanism. *Nature Structural & Molecular Biology*, *19*(2), 253–259. https://doi.org/10.1038/nsmb.2223

Dowers, E., Zamora, F., Barakat, L. A., & Ogbuagu, O. (2018). Dolutegravir/rilpivirine for the treatment of HIV-1 infection. *HIV AIDS (Auckl)*, *10*, 215–224. https://doi.org/10.2147/HIV.S157855

Feng, M., Wang, D., Grobler, J. A., Hazuda, D. J., Miller, M. D., & Lai, M. T. (2015). In vitro resistance selection with doravirine (MK-1439), a novel nonnucleoside reverse transcriptase inhibitor with distinct mutation development pathways. *Antimicrobial Agents and Chemotherapy*, *59*(1), 590–598. https://doi.org/10.1128/AAC.04201-14

Gathe, J., Andrade-Villanueva, J., Santiago, S., Horban, A., Nelson, M., Cahn, P., … Quinson, A. M. (2011). Efficacy and safety of nevirapine extended-release once daily versus nevirapine immediate-release twice-daily in treatment-naive HIV-1-infected patients. *Antiviral Therapy*, *16*(5), 759–769. https://doi.org/10.3851/IMP1803

Gibson, K. M., Steiner, M. C., Kassaye, S., Maldarelli, F., Grossman, Z., Perez-Losada, M., & Crandall, K. A. (2019). A 28-year history of HIV-1 drug resistance and transmission in Washington, DC. *Frontiers in Microbiology*, *10*, 369. https://doi.org/10.3389/fmicb.2019.00369

Gu, S. X., Lu, H. H., Liu, G. Y., Ju, X. L., & Zhu, Y. Y. (2018). Advances in diarylpyrimidines and related analogues as HIV-1 nonnucleoside reverse transcriptase inhibitors. *European Journal of Medicinal Chemistry*, *158*, 371–392. https://doi.org/10.1016/j.ejmech.2018.09.013

Gulick, R. M. (2018). Investigational antiretroviral drugs: What is coming down the pipeline. *Topics in Antiviral Medicine*, *25*(4), 127–132.

Gulick, R. M., & Flexner, C. (2019). Long-acting HIV drugs for treatment and prevention. *Annual Review of Medicine*, *70*, 137–150. https://doi.org/10.1146/annurev-med-041217-013717

Havlir, D., McLaughlin, M. M., & Richman, D. D. (1995). A pilot study to evaluate the development of resistance to nevirapine in asymptomatic human immunodeficiency virus-infected patients with CD4 cell counts of >500/mm^3: AIDS Clinical Trials Group Protocol 208. *Journal of Infectious Diseases*, *172*(5), 1379–1383. https://doi.org/10.1093/infdis/172.5.1379

Huang, B., Chen, W., Zhao, T., Li, Z., Jiang, X., Ginex, T., … Liu, X. (2019). Exploiting the tolerant region I of the non-nucleoside reverse transcriptase inhibitor (NNRTI) binding pocket: Discovery of potent diarylpyrimidine-typed HIV-1 NNRTIs against wild-type and E138K mutant virus with significantly improved water solubility and favorable safety profiles. *Journal of Medicinal Chemistry*, *62*(4), 2083–2098. https://doi.org/10.1021/acs.jmedchem.8b01729

Johnson, B. C., Pauly, G. T., Rai, G., Patel, D., Bauman, J. D., Baker, H. L., … Hughes, S. H. (2012). A comparison of the ability of rilpivirine (TMC278) and selected analogues to inhibit clinically relevant HIV-1 reverse transcriptase mutants. *Retrovirology*, *9*, 99. https://doi.org/10.1186/1742-4690-9-99

Kang, D., Wang, Z., Chen, M., Feng, D., Wu, G., Zhou, Z., … Liu, X. (2019). Discovery of potent HIV-1 non-nucleoside reverse transcriptase inhibitors by exploring the structure-activity relationship of solvent-exposed regions I. *Chemical Biology & Drug Design*, *93*(4), 430–437. https://doi.org/10.1111/cbdd.13429

Kang, D., Zhang, H., Wang, Z., Zhao, T., Ginex, T., Luque, F. J., … Liu, X. (2019). Identification of dihydrofuro[3,4-d]pyrimidine derivatives as novel HIV-1 non-nucleoside reverse transcriptase inhibitors with promising antiviral activities and desirable physicochemical properties. *Journal of Medicinal Chemistry*, *62*(3), 1484–1501. https://doi.org/10.1021/acs.jmedchem.8b01656

Liu, N., Wei, L., Huang, L., Yu, F., Zheng, W., Qin, B., … Xie, L. (2016). Novel HIV-1 non-nucleoside reverse transcriptase inhibitor agents: optimization of diarylanilines with high potency against wild-type and rilpivirine-resistant E138K mutant virus. *Journal of Medicinal Chemistry*, *59*(8), 3689–3704. https://doi.org/10.1021/acs.jmedchem.5b01827

Llibre, J. M., Hung, C. C., Brinson, C., Castelli, F., Girard, P. M., Kahl, L. P., … Aboud, M. (2018). Efficacy, safety, and tolerability of dolutegravir-rilpivirine for the maintenance of virological suppression in adults with HIV-1: Phase 3, randomised, non-inferiority SWORD-1 and SWORD-2 studies. *The Lancet*, *391*(10123), 839–849. https://doi.org/10.1016/S0140-6736(17)33095-7

Maldarelli, F., Palmer, S., King, M. S., Wiegand, A., Polis, M. A., Mican, J., … Mellors, J. W. (2007). ART suppresses plasma HIV-1 RNA to a stable set point predicted by pretherapy viremia. *PLoS Path*, *3*(4), e46. https://doi.org/10.1371/journal.ppat.0030046

Margolis, A. M., Heverling, H., Pham, P. A., & Stolbach, A. (2014). A review of the toxicity of HIV medications. *Journal of Medical Toxicology*, *10*(1), 26–39. https://doi.org/10.1007/s13181-013-0325-8

Margolis, D. A., Brinson, C. C., Smith, G. H. R., de Vente, J., Hagins, D. P., Eron, J. J., … Team, L. A. I. S. (2015). Cabotegravir plus rilpivirine, once a day, after induction with cabotegravir plus nucleoside reverse transcriptase inhibitors in antiretroviral-naive adults with HIV-1 infection (LATTE): A randomised, phase 2b, dose-ranging trial. *The Lancet Infectious Diseases*, *15*(10), 1145–1155. https://doi.org/10.1016/S1473-3099(15)00152-8

Margolis, D. A., Gonzalez-Garcia, J., Stellbrink, H. J., Eron, J. J., Yazdanpanah, Y., Podzamczer, D., … Spreen, W. R. (2017). Long-acting intramuscular cabotegravir and rilpivirine in adults with

HIV-1 infection (LATTE-2): 96-week results of a randomised, open-label, phase 2b, non-inferiority trial. *The Lancet*, *390*(10101), 1499–1510. https://doi.org/10.1016/S0140-6736(17)31917-7

Mayer, K. H., Hosek, S., Cohen, S., Liu, A., Pickett, J., Warren, M., … Grant, R. (2015). Antiretroviral pre-exposure prophylaxis implementation in the United States: A work in progress. *Journal of the International AIDS Society*, *18*(4 Suppl. 3), 19980. https://doi.org/10.7448/IAS.18.4.19980

McCormack, S., Dunn, D. T., Desai, M., Dolling, D. I., Gafos, M., Gilson, R., … Gill, O. N. (2016). Pre-exposure prophylaxis to prevent the acquisition of HIV-1 infection (PROUD): Effectiveness results from the pilot phase of a pragmatic open-label randomised trial. *The Lancet*, *387*(10013), 53–60. https://doi.org/10.1016/S0140-6736(15)00056-2

Namasivayam, V., Vanangamudi, M., Kramer, V. G., Kurup, S., Zhan, P., Liu, X., … Byrareddy, S. N. (2019). The journey of HIV-1 non-nucleoside reverse transcriptase inhibitors (NNRTIs) from lab to clinic. *Journal of Medicinal Chemistry*, *62*(10), 4851–4883. https://doi.org/10.1021/acs.jmedchem.8b00843

Pasquau, J., de Jesus, S. E., Arazo, P., Crusells, M. J., Rios, M. J., & Lozano, F., … on behalf of the RIDAR Study Group. (2019). Effectiveness and safety of dual therapy with rilpivirine and boosted darunavir in treatment-experienced patients with advanced HIV infection: A preliminary 24 week analysis (RIDAR study). *BMC Infectious Diseases*, *19*(1), 207. https://doi.org/10.1186/s12879-019-3817-6

Perelson, A. S., Essunger, P., Cao, Y., Vesanen, M., Hurley, A., Saksela, K., … Ho, D. D. (1997). Decay characteristics of HIV-1-infected compartments during combination therapy. *Nature*, *387*(6629), 188–191. https://doi.org/10.1038/387188a0

Ren, J., Bird, L. E., Chamberlain, P. P., Stewart-Jones, G. B., Stuart, D. I., & Stammers, D. K. (2002). Structure of HIV-2 reverse transcriptase at 2.35-A resolution and the mechanism of resistance to non-nucleoside inhibitors. *Proceedings of the National Academy of Sciences USA*, *99*(22), 14410–14415. https://doi.org/10.1073/pnas.222366699

Schils, D., Stappers, F., Solberghe, G., van Heck, R., Coppens, M., Van den Heuvel, D., … Schouteden, E. (2008). Ligandless heck coupling between a halogenated aniline and acrylonitrile catalyzed by Pd/C: Development and optimization of an industrial-scale heck process for the production of a pharmaceutical intermediate. *Organic Process Research & Development*, *12*(3), 530–536. https://doi.org/10.1021/op8000383

Scott, L. J., & Perry, C. M. (2000). Delavirdine: A review of its use in HIV infection. *Drugs*, *60*(6), 1411–1444. https://doi.org/10.2165/00003495-200060060-00013

Shafer, R. W., Smeaton, L. M., Robbins, G. K., De Gruttola, V., Snyder, S. W., D'Aquila, R. T., … the AIDS Clinical Trials Group 384 Team (2003). Comparison of four-drug regimens and pairs of sequential three-drug regimens as initial therapy for HIV-1 infection. *New England Journal of Medicine*, *349*(24), 2304–2315. https://doi.org/10.1056/NEJMoa030265

Sluis-Cremer, N., & Tachedjian, G. (2008). Mechanisms of inhibition of HIV replication by non-nucleoside reverse transcriptase inhibitors. *Virus Research*, *134*(1–2), 147–156. https://doi.org/10.1016/j.virusres.2008.01.002

Smith, S. J., & Hughes, S. H. (2014). Rapid screening of HIV reverse transcriptase and integrase inhibitors. *Journal of Visualized Experiments*, *86*(51400). https://doi.org/10.3791/51400

Smith, S. J., Pauly, G. T., Akram, A., Melody, K., Ambrose, Z., Schneider, J. P., & Hughes, S. H. (2016). Rilpivirine and doravirine have complementary efficacies against NNRTI-resistant HIV-1 Mutants. *Journal of Acquired Immune Deficiency Syndromes*, *72*(5), 485–491. https://doi.org/10.1097/QAI.0000000000001031

Smith, S. J., Pauly, G. T., Akram, A., Melody, K., Rai, G., Maloney, D. J., … Hughes, S. H. (2016). Rilpivirine analogs potently inhibit drug-resistant HIV-1 mutants. *Retrovirology*, *13*, 11. https://doi.org/10.1186/s12977-016-0244-2

Smith, S. J., Zhao, X. Z., Burke, T. R. Jr., & Hughes, S. H. (2018). HIV-1 integrase inhibitors that are broadly effective against drug-resistant mutants. *Antimicrobial Agents and Chemotherapy*, *62*(9), e01035–18. https://doi.org/10.1128/AAC.01035-18

Tebit, D. M., Lobritz, M., Lalonde, M., Immonen, T., Singh, K., Sarafianos, S., … Arts, E. J. (2010). Divergent evolution in reverse transcriptase (RT) of HIV-1 group O and M lineages: Impact on structure, fitness, and sensitivity to nonnucleoside RT inhibitors. *Journal of Virology*, *84*(19), 9817–9830. https://doi.org/10.1128/JVI.00991-10

Wang, Y., De Clercq, E., & Li, G. (2019). Current and emerging non-nucleoside reverse transcriptase inhibitors (NNRTIs) for HIV-1 treatment. *Expert Opinion on Drug Metabolism & Toxicology*, *15*(10), 813–829. https://doi.org/10.1080/17425255.2019.1673367

Wensing, A. M., Calvez, V., Ceccherini-Silberstein, F., Charpentier, C., Gunthard, H. F., Paredes, R., … Richman, D. D. (2019). 2019 update of the drug resistance mutations in HIV-1. *Topics in Antiviral Medicine*, *27*(3), 111–121.

Xavier Ruiz, F., & Arnold, E. (2020). Evolving understanding of HIV-1 reverse transcriptase structure, function, inhibition, and resistance. *Current Opinion in Structural Biology*, *61*, 113–123. https://doi.org/10.1016/j.sbi.2019.11.011

SUPPORTING INFORMATION

Additional supporting information may be found online in the Supporting Information section.

How to cite this article: Smith SJ, Pauly GT, Hewlett K, Schneider JP, Hughes SH. Structure-based non-nucleoside inhibitor design: Developing inhibitors that are effective against resistant mutants. *Chem Biol Drug Des*. 2021;97:4–17. https://doi.org/10.1111/cbdd.13766